

Qualitative and Quantitative Analyses of Synthesized Short-Chain Fatty Acid Phenyl Esters Using Fourier-Transform Infrared Spectroscopy

Ronald P. D'Amelia*, Masashi W. Kimura, Marie-Claire Villon

Chemistry Department, Hofstra University, Hempstead, NY

*Corresponding author: Ronald.p.damelia@hofstra.edu

Received May 22, 2021; Revised June 28, 2021; Accepted July 08, 2021

Abstract Fourier-transform infrared spectroscopy (FT-IR) is a widely used technique to qualitatively determine the molecular structure of organic compounds; however, using quantitative FT-IR (qFT-IR) for the compositional analyses of mixtures is less common. To reinforce instrumental use in undergraduate laboratories, we have devised a multipart experiment that not only combines the qualitative and quantitative aspects of FT-IR but also exposes students to computational and synthetic organic chemistry. The objectives of this experiment are to synthesize a series of phenyl esters (PhEs) of various molecular weights; use qualitative FT-IR to characterize and compare the synthesized products with standards, databases, and with theoretical spectra computed using the cost-efficient B97-3c functional; and determine the weight percent (wt. %) composition of a binary mixture. We report on the methodologies used to synthesize and purify four PhEs; characterize them using FT-IR, conduct theoretical calculations and compare their FT-IR spectra with experimental ones; and determine the wt. % composition of phenyl acetate (PhAc), phenyl propionate (PhPr), phenyl butyrate (PhBu), and phenyl hexanoate (PhHex) in binary mixtures ranging from 0% to 100%. The results show a strong, linear correlation of gravimetrically calculated wt. % composition of a selected compound in a binary mixture using qFT-IR. This experiment demonstrates the applicability of qFT-IR as an educational tool for the undergraduate chemical laboratory and combines four different branches of chemistry: computational, instrumental, organic, and analytical.

Keywords: *ab initio*, computational chemistry, density functional theory, esterification, Fourier-transform infrared spectroscopy, hands-on learning, phenyl esters, phenyl ester mixtures, quantitative analysis, synthetic organic chemistry, undergraduate laboratory experimente

Cite This Article: Ronald P. D'Amelia, Masashi W. Kimura, and Marie-Claire Villon, "Qualitative and Quantitative Analyses of Synthesized Short-Chain Fatty Acid Phenyl Esters Using Fourier-Transform Infrared Spectroscopy." *World Journal of Organic Chemistry*, vol. 9, no. 1 (2021): 6-17. doi: 10.12691/wjoc-9-1-2.

1. Introduction

Infrared (IR) spectroscopy is a common technique routinely taught in many undergraduate chemistry courses, and regularly used for both qualitative and quantitative analyses [1-9]. With the increase in signal-to-noise ratio, Fourier-transform infrared spectroscopy (FT-IR) has become one of the most essential instruments to determine chemical structure and composition. The latter often refers to quantitative FT-IR (qFT-IR), where its utilization has been well documented for the compositional analyses of different fatty acids [10-18]. Since we have previously used qFT-IR for the compositional analyses of various copolymers and blends and sought to increase exposure to FT-IR techniques in the undergraduate laboratories, we have developed an experiment that uses instrumental, synthetic, and computational techniques. [19,20].

FT-IR exploits the quantized nature of photonic absorption in molecules, where different functional groups

absorb IR light at certain frequencies, resulting in either stretching or bending movements specific to those groups [21,22]. These vibrations are also associated with changes in electric dipole moments. Symmetrical molecules, such as homonuclear diatomic gases, often yield no changes in dipole moments when they absorb infrared light, and, therefore, are unobservable on an FT-IR spectrum. An FT-IR spectrum generally plots transmission (or absorption) versus frequency, where each peak is characteristic to a specific functional group. The intensities of these peaks are also proportional to the concentration of the molecule according to Beer's Law.

Using *ab initio* methods to simulate FT-IR spectra is achievable; in fact, it has become a common practice to compare theoretical spectra with their experimental counterparts [23-28]. Unfortunately, the main downsides of using these methods are computational costs along with accuracy. Many *ab initio* methods, including density functional theory (DFT), are computationally expensive, and theoretical spectra often need scaling factors to accurately replicate their experimental counterparts [29,30,31].

Nevertheless, modern theoretical methods are constantly evolving, and the development of neural networks may

lead to accurate and real-time results, which would be ideal for both industrial and academic applications [32,33,34].

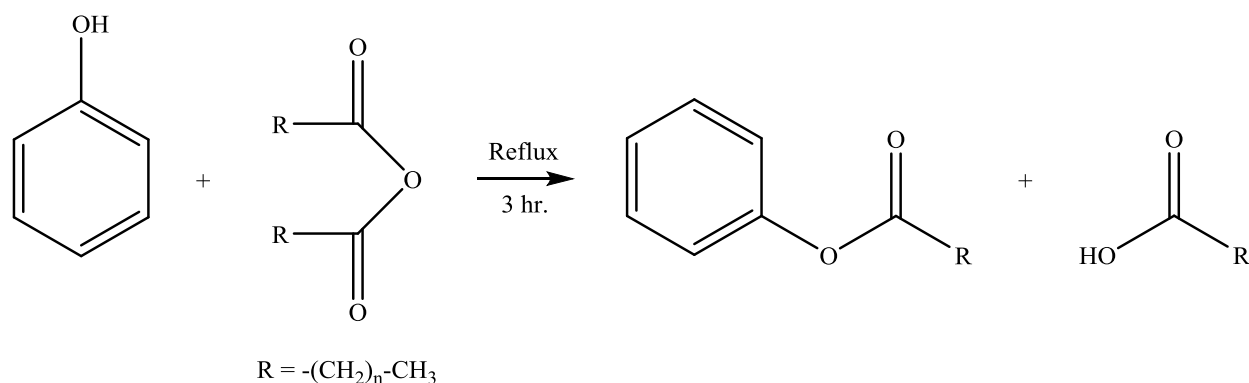


Figure 1. Reaction Scheme of PhE and its Carboxylic Acid Byproduct from PhOH and an Acid Anhydride

There are multiple objectives to our experiment. The first is to synthesize four different phenyl esters (PhEs) of various molecular weights. These include phenyl acetate (PhAc), phenyl propionate (PhPr), phenyl butyrate (PhBu), and phenyl hexanoate (PhHex). These PhEs were synthesized via esterification of phenol (PhOH) and their corresponding acid anhydrides. The second is to characterize each PhE by comparing their FT-IR spectra to standards, spectral databases, and computational simulations. The third is to prepare a series of binary mixtures containing two different PhEs ranging from 20% to 80% by volume. Pure PhEs shall represent either 0% or 100%. The weight percent (wt. %) composition of each binary mixture was also determined gravimetrically. The fourth is to construct calibration curves of each binary mixture by plotting the average FT-IR integration of a peak, or over a frequency range, versus the gravimetrically determined wt. % composition of a PhE. Lastly, the fifth is to determine the wt. % composition of an unknown binary mixture.

1.1. Learning Objectives

1. To understand the overall principles of FT-IR.
2. To learn how to synthesize various PhEs via esterification of PhOH and their corresponding acid anhydrides, and properly prepare binary mixtures using volumetric and gravimetric techniques.
3. To characterize each PhE by determining the functional groups associated with each FT-IR peak, and compare them to standards, spectral databases, and computational simulations.
4. To establish correlation curves between the integrated FT-IR peak areas, or over a range of frequencies, and the gravimetric wt. % compositions for each binary mixture.

2. Materials and Methods

2.1. Student Procedure

Each student shall be assigned a PhE to synthesize using PhOH and its corresponding acid anhydride. They would then proceed to purify them by neutralizing the acid byproduct. Figure 1 provides a general reaction scheme of

a PhE. They will then characterize their pure product using FT-IR and compare them to standards, spectral databases, or computational simulations. The instructor or students shall perform DFT computations to generate the theoretical FT-IR spectra of each PhE. The instructor will assign each student to prepare binary mixtures of approximately 20%, 40%, 60%, and 80% by volume. Sample vials (7-mL) will be weighed before and after the addition of a PhE, and this will be repeated for the second PhE. All recorded weights will be used to compute the wt. % composition of each component. Students will run FT-IR on their samples, where they will construct calibration curves of the average FT-IR integrations and the gravimetric wt. % composition of a component. Afterward, the students will receive an unknown sample prepared by the instructor, where they must determine the wt. % composition of a selected component.

2.2. Experimental Materials

Phenol ($\geq 99.0\%$ pure), acetic anhydride (99% pure), propionic anhydride (99% pure), butyric anhydride (98% pure), hexanoic anhydride (97% pure), sodium bicarbonate ($\geq 99.5\%$ pure), and phenyl propionate (99% pure) were supplied by Sigma-Aldrich™. Anhydrous sodium sulfate ($\geq 99.0\%$ pure) was supplied by Macron Fine Chemicals™.

2.2.1. Synthesis of PhEs

Approximately 10 grams of PhOH was weighed into a 100-mL three-neck, round-bottom flask fitted with a condenser, thermometer, and a 100-mL addition funnel. Approximately 15-mL of an acid anhydride (acetic, propionic, butyric, or hexanoic) was added to the round-bottom flask. The acid anhydride was added slowly with stirring, and the solution was refluxed for around three hours at different temperatures depending on the anhydride (125 °C for acetic, 140 °C for propionic, 150 °C for butyric, and 250 °C for hexanoic). After reflux, approximately 25-mL of distilled water was added to neutralize the excess anhydride. This solution was poured into a 250-mL separatory funnel, which was capped and inverted several times. The aqueous layer was removed and neutralized with sodium bicarbonate, while the PhE was transferred to a 250-mL round-bottom flask. Approximately 100-mL of

a saturated sodium bicarbonate solution was slowly added with stirring, and the solution was left alone for around an hour. Afterward, the solution was poured into a 250-mL separatory funnel, where the aqueous layer was removed, while the PhE was transferred to a labeled 20-mL scintillation vial. Some anhydrous sodium sulfate was added to the vial, and after a day, the PhE was transferred to a new, labeled, and pre-weighed 20-mL scintillation vial, which was then weighed and analyzed using FT-IR.

2.2.2. Preparation of Binary PhE Mixtures

Twelve, 200- μ L mixtures of PhEs were made as shown in Table 1. All 7-mL vials were labeled based on the volumetric ratio in the mixture and weighed before adding any PhE. Each PhE was added using a Gilson classic model P200 pipette. After each addition of a PhE into a vial, their masses were recorded using an analytical balance with a 0.1-mg precision. These masses were used to calculate wt. % composition of a component in each binary mixture using equation 1:

$$\% \text{ composition} = \frac{N_X}{N_X + N_Y} * 100 \quad (1)$$

where N_X and N_Y are the gravimetrically determined masses of each component in a mixture.

For the unknowns, a 50:50 mixture of PhAc-PhPr, PhAc-PhBu, and PhAc-PhHex was prepared by the instructor as shown in Table 2.

2.2.3. Fourier-Transform Infrared Spectroscopy (FT-IR)

All PhE samples were analyzed using a Bruker Alpha-P FT-IR spectrometer with a Platinum® attenuated total internal reflectance quick snap module with a diamond crystal. The Alpha-P had a Michelson Interferometer with a SiC globar as the IR source, and the time dependence of the IR intensity was measured with a pyroelectric DTGS detector. The data analyses were done using the Bruker OPUS® software version 7.0.122. Background measurements were conducted with 48 scans and a resolution of 2 cm^{-1} . Approximately 20- μ L of each sample was analyzed by simply pressing the droplet between the anvil and diamond crystal. Each measurement represents the average spectrum of the aforementioned number of scans and resolution used for the background measurement. For qFT-IR measurements, five scans were conducted for each sample and their peak integrations were obtained using the built-in integration feature.

Table 1. Summary of Aliquoted Binary Mixtures

Volumetric Ratio	
Phenyl Acetate: Phenyl Propionate	Gravimetrically Determined wt. % Phenyl Acetate
0 μ L: 200 μ L PhAc: PhPr	0.0
40 μ L: 160 μ L PhAc: PhPr	12.9
80 μ L: 120 μ L PhAc: PhPr	27.7
120 μ L: 80 μ L PhAc: PhPr	58.3
160 μ L: 40 μ L PhAc: PhPr	67.0
200 μ L: 0 μ L PhAc: PhPr	100.0
Phenyl Acetate: Phenyl Butyrate	Gravimetrically Determined wt. % Phenyl Acetate
0 μ L: 200 μ L PhAc: PhBu	0.0
40 μ L: 160 μ L PhAc: PhBu	15.7
80 μ L: 120 μ L PhAc: PhBu	46.9
120 μ L: 80 μ L PhAc: PhBu	52.9
160 μ L: 40 μ L PhAc: PhBu	72.8
200 μ L: 0 μ L PhAc: PhBu	100.0
Phenyl Acetate: Phenyl Hexanoate	Gravimetrically Determined wt. % Phenyl Acetate
0 μ L: 200 μ L PhAc: PhHex	0.0
40 μ L: 160 μ L PhAc: PhHex	19.8
80 μ L: 120 μ L PhAc: PhHex	41.4
120 μ L: 80 μ L PhAc: PhHex	48.0
160 μ L: 40 μ L PhAc: PhHex	84.0
200 μ L: 0 μ L PhAc: PhHex	100.0

Table 2. Summary of Aliquoted Unknown Binary Mixtures

Volumetric Ratio	
Phenyl Acetate: Phenyl Propionate	Gravimetrically Determined wt. % Phenyl Acetate
200 μ L: 200 μ L PhAc: PhPr	50.73
Phenyl Acetate: Phenyl Butyrate	Gravimetrically Determined wt. % Phenyl Acetate
200 μ L: 200 μ L PhAc: PhBu	52.01
Phenyl Acetate: Phenyl Hexanoate	Gravimetrically Determined wt. % Phenyl Acetate
200 μ L: 200 μ L PhAc: PhHex	52.67

2.2.4. Theoretical Methods

Each PhE was modeled using the Avogadro software package to initially optimize its geometry using the universal force field method and generate the necessary input files [35,36,37]. DFT calculations were conducted using the ORCA software package, version 4.2.1, and the cost-efficient B97-3c functional with the def2-mTZVP basis set [38,39]. Geometry optimization was first conducted, followed by an analytical frequency calculation. Both calculations were performed in the gas phase. The necessary theoretical FT-IR data were generated using the built-in "orca_mapspc" feature to convert an output file into data points with a specified wavenumber range of 4000-400 cm^{-1} . Theoretical FT-IR spectra were constructed by plotting transmission vs. wavenumber (cm^{-1}); data points from the experimentally obtained FT-IR spectra were also plotted for comparison.

2.2.5. Hazards

Students are required to wear gloves and safety glasses during the entirety of the experiment. Acid anhydrides are flammable, corrosive, and water-sensitive chemicals, which should be handled exclusively in a fume hood. Sodium bicarbonate is not classified as a hazardous material; however, it can cause slight skin and eye irritations upon contact. Anhydrous sodium sulfate is very

hygroscopic, and it may cause eye, skin, and respiratory tract irritation upon contact.

2.2.6. Statistical Analysis

Each of the binary mixtures was analyzed multiple times. The data reported is the average of the normalized peak areas. The average percent relative standard deviation for the analyzed samples ranged from 0.34% to 2.26%. Propagation of error analyses was conducted for all calibration plots and for calculating the experimental wt. % composition of a component in a 50:50 mixture. All gravimetric wt. % compositions were within the 95% confidence interval (CI) of the experimental results for five measurements.

3. Results and Discussion

3.1. FT-IR Analysis of PhEs

All qualitative FT-IR analyses of the PhEs were conducted using transmission measurements. Figure 2 showcases the overlapping spectra of all PhEs. Table 3 summarizes the IR vibrations for all PhEs. Stretching and bending vibrations are represented by lowercases nu (ν) and delta (δ), respectively.



Figure 2. Overlapped FT-IR Spectra of PhEs

Table 3. Summary of FT-IR Data of PhEs Reported in Wavenumbers (cm^{-1}).

Functional Group	Type of Vibration	PhAc	PhPr	PhBu	PhHex
Aromatic	$\nu\text{C-H}$	3044	3044	3044	3044
Aliphatic	$\nu\text{C-H}$	---	2983	2967	2956
Aliphatic	$\nu\text{C-H}$	---	2943	2936	2932
Aliphatic	$\nu\text{C-H}$	---	2884	2876	2872
Ester	$\nu\text{C=O}$	1761	1758	1754	1759
Aromatic	$\nu\text{C=C}$	1593	1593	1593	1593
Aromatic	$\nu\text{C=C}$	1492	1493	1493	1493
Aliphatic	$\delta\text{C-H}$	---	---	---	1467
Aliphatic	$\delta\text{C-H}$	1457	1457	1457	1457
Aliphatic	$\delta\text{C-H}$	1431	1421	1416	1417
Aliphatic	$\delta\text{C-H}$	---	---	---	1378
Aliphatic	$\delta\text{C-H}$	1369	1353	1364	1364
Aliphatic	$\delta\text{C-H}$	---	---	1347	---
Aliphatic	$\delta\text{C-H}$	---	---	---	1315
Aliphatic	$\delta\text{C-H}$	1290	---	1301	1294
Aliphatic	$\delta\text{C-H}$	---	1268	---	---
Ester	$\nu\text{C-O}$	---	---	1243	---
Ester	$\nu\text{C-O}$	1212	---	---	---
Ester	$\nu\text{C-O}$	---	1193	1194	1194
Ester	$\nu\text{C-O}$	1184	---	---	---
Ester	$\nu\text{C-O}$	1161	1162	1161	1162
Ester	$\nu\text{C-O}$	---	1136	1140	1139
Ester	$\nu\text{C-O}$	---	---	1097	1101
Ester	$\nu\text{C-O}$	1069	1071	1071	1070
Ester	$\nu\text{C-O}$	1045	---	---	---
Ester	$\nu\text{C-O}$	---	---	1033	---
Ester	$\nu\text{C-O}$	1026	1024	1024	1024
Ester	$\nu\text{C-O}$	1012	---	---	---
Ester	$\nu\text{C-O}$	1006	1005	1007	1007
Aromatic	$\delta\text{C-H}$	---	979	---	---
Aromatic	$\delta\text{C-H}$	923	916	928	932
Aromatic	$\delta\text{C-H}$	---	---	908	916
Aromatic	$\delta\text{C-H}$	891	872	886	876
Aromatic	$\delta\text{C-H}$	814	806	811	813
Aromatic	$\delta\text{C-H}$	---	---	765	---
Aromatic	$\delta\text{C-H}$	747	752	745	750
Aromatic	$\delta\text{C-H}$	---	---	712	708
Aromatic	$\delta\text{C-H}$	690	690	688	688
Aromatic	$\delta\text{C=C}$	663	---	---	---
Aromatic	$\delta\text{C=C}$	---	614	---	614
Aromatic	$\delta\text{C=C}$	594	---	---	---
Aromatic	$\delta\text{C=C}$	529	521	---	537
Aromatic	$\delta\text{C=C}$	498	498	499	498

All PhEs have a weak aromatic $\nu\text{C-H}$ peak at approximately 3044 cm^{-1} , two $\nu\text{C=C}$ peaks at approximately 1593 cm^{-1} and 1492 cm^{-1} , and multiple aromatic $\delta\text{C-H}$ and $\delta\text{C=C}$ peaks between $980\text{-}490\text{ cm}^{-1}$, which are characteristic of the phenyl group. All PhEs also have a strong $\nu\text{C=O}$ peak at approximately 1758 cm^{-1} , and multiple $\nu\text{C-O}$ peaks between $1220\text{-}1000\text{ cm}^{-1}$, which are characteristic of the ester group; and multiple aliphatic $\delta\text{C-H}$ peaks between $1470\text{-}1250\text{ cm}^{-1}$, which are characteristic of the methyl and methylene groups. PhPr, PhBu, and PhHex have additional $\nu\text{C-H}$ peaks between

$2990\text{-}2850\text{ cm}^{-1}$ that increase in absorption intensity as more methylenes are added to the aliphatic tail.

Figure 3 is a correlation plot of the FT-IR frequencies from the synthesized PhPr and its standard that was purchased from Sigma-Aldrich™. Figure 4 compares experimentally obtained FT-IR frequencies to those reported in the Spectral Database for Organic Compounds (SDBS) for PhAc, PhPr, and PhBu [40]. The correlation plots in both Figure 3 and Figure 4 demonstrate that there are excellent agreements, as indicated by the correlation coefficients (R^2) being 1.

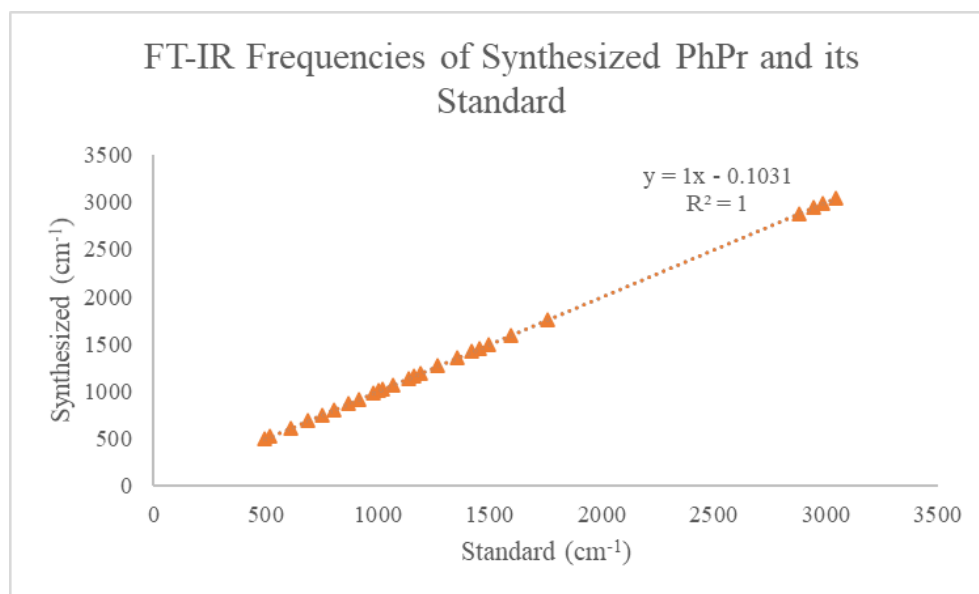


Figure 3. Correlation Plot of the FT-IR Frequencies from the Synthesized PhPr and its Standard Purchased from Sigma-Aldrich™

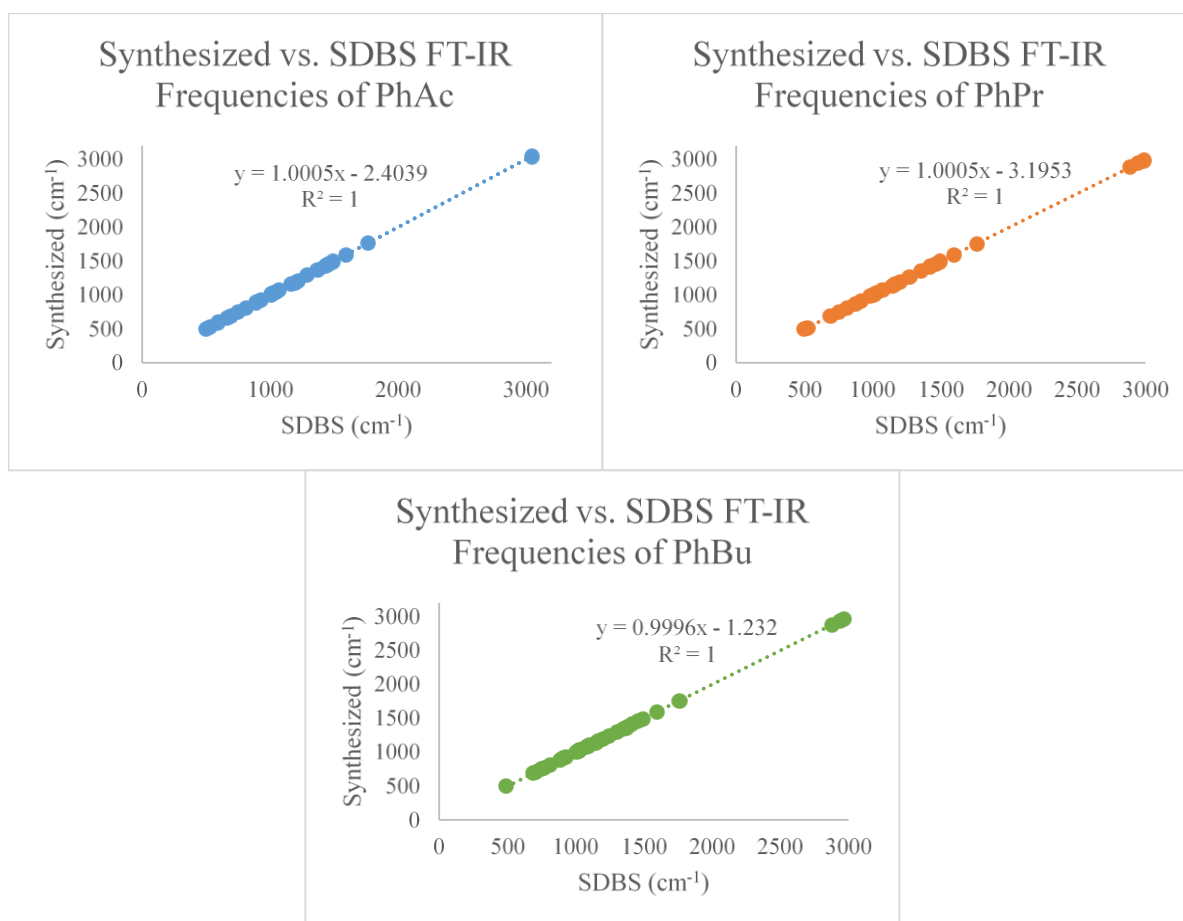


Figure 4. Correlation Plots of FT-IR Frequencies Obtained Experimentally and from SDBS for PhAc (Blue, Top Left), PhPr (Orange, Top Right), and PhBu (Green, Bottom Middle)

3.2. Assessment of Theoretical FT-IR Calculations using B97-3c

Figure 5 shows the correlation plots of the experimentally obtained FT-IR frequencies versus those calculated using the B97-3c functional in the gas phase. In all cases, there are strong, linear agreements between the experimentally

obtained and theoretically computed FT-IR frequencies. All cases have R^2 values greater than 0.999. Scaling factors could also be acquired from these plots, which could improve the accuracy of the computed frequencies [29,30,31]. Scaling factors can be applied using equation 2:

$$\nu_{Scaled} = A * \nu_{Computed} + B \quad (2)$$

where A is the slope and B is the y-intercept of a correlation plot specific to a PhE. Additionally, these scaling factors and their uncertainties could be averaged together and applied to all PhEs, which results in $A = 0.9539 \pm 0.0021$ and $B = 42.87 \pm 3.11 \text{ cm}^{-1}$. These new scaling factors were applied to all computed

B97-3c frequencies, which were plotted with their respective experimental FT-IR spectra in Figure 6 through 9 for comparison. Overall, the B97-3c functional offers an affordable and accurate prediction of IR frequencies to confirm the structure of each PhE.

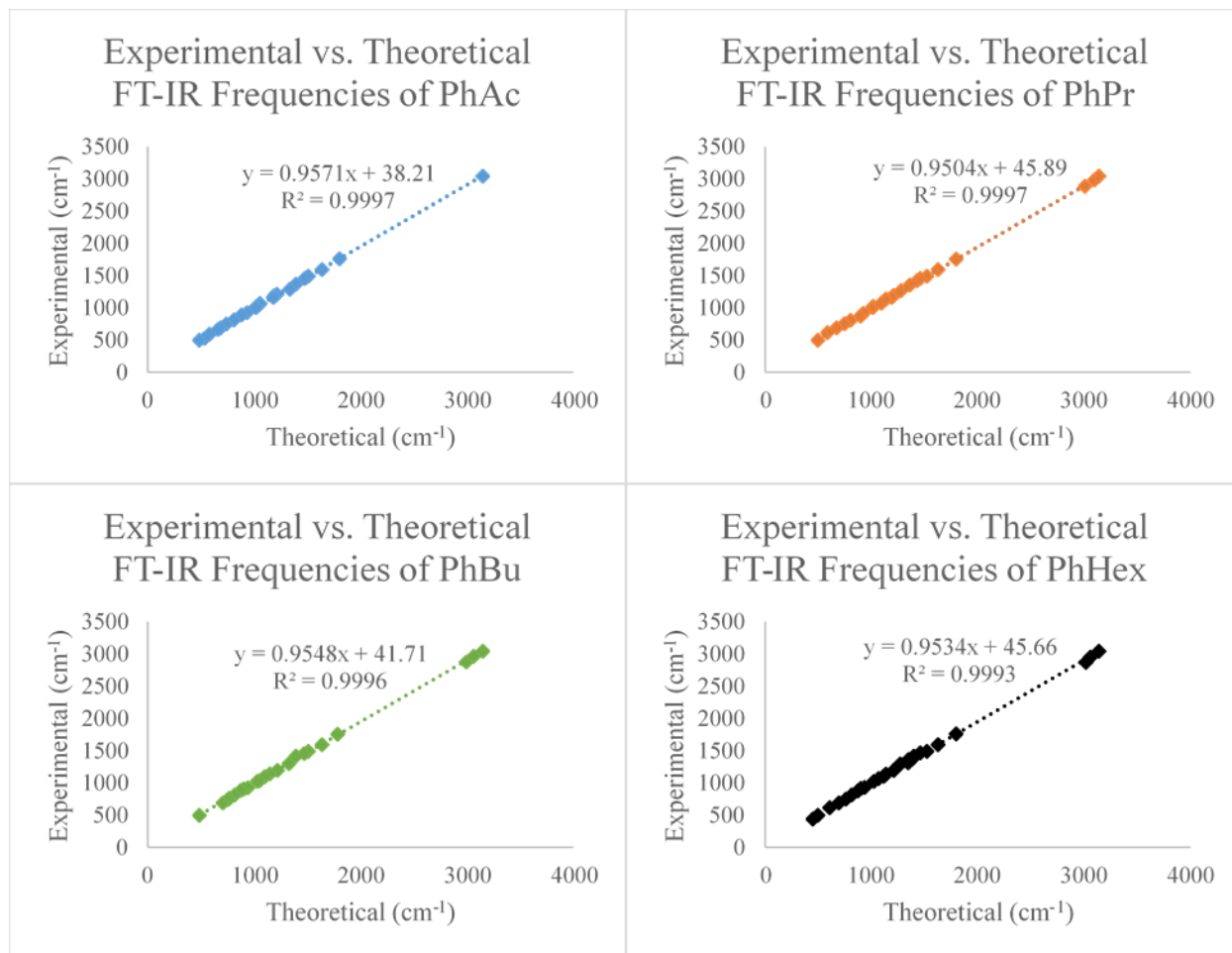


Figure 5. Correlation Plots of FT-IR Frequencies Obtained Experimentally and from Theoretical Calculations using the B97-3c Functional for PhAc (Blue, Top Left), PhPr (Orange, Top Right), PhBu (Green, Bottom Left), and PhHex (Black, Bottom Right)

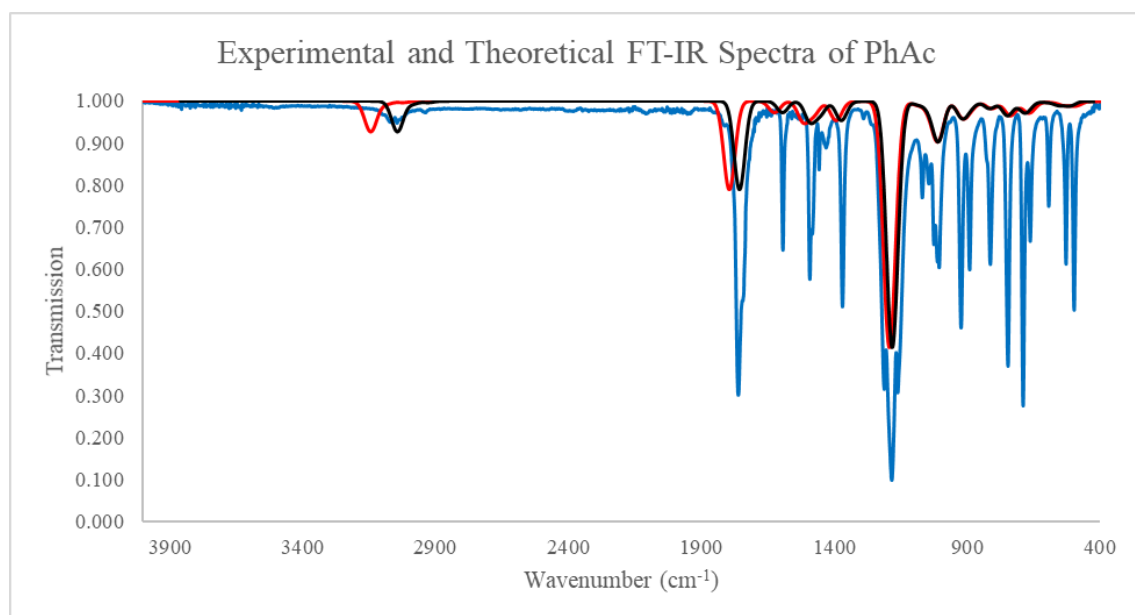


Figure 6. FT-IR Spectra of PhAc Experimental (Blue), Theoretical using B97-3c (Red), and B97-3c with Scaling Factors (Black)

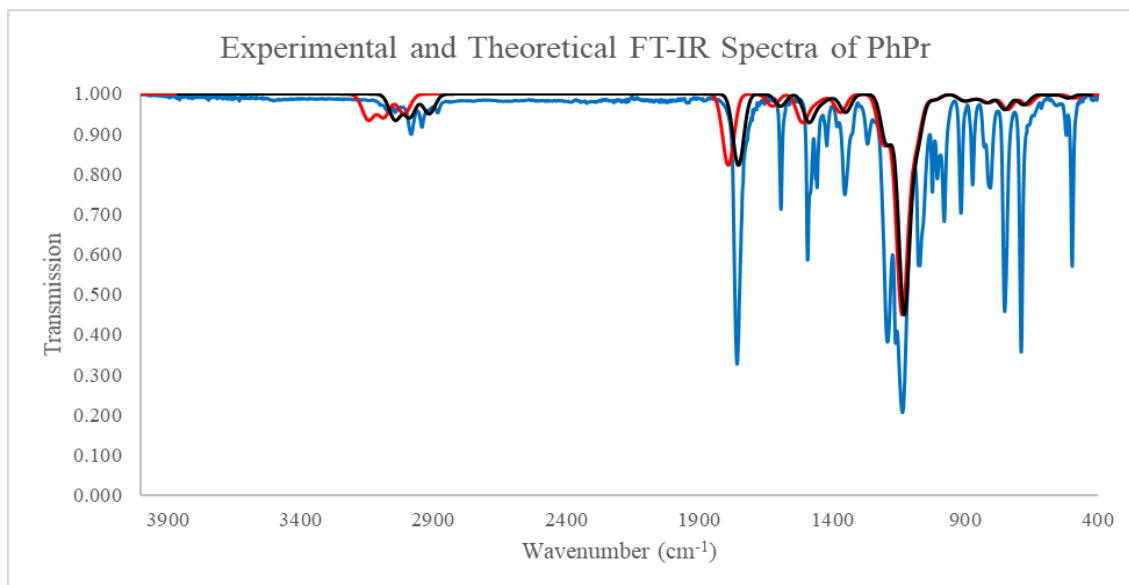


Figure 7. FT-IR Spectra of PhPr Experimental (Blue), Theoretical using B97-3c (Red), and B97-3c with Scaling Factors (Black)

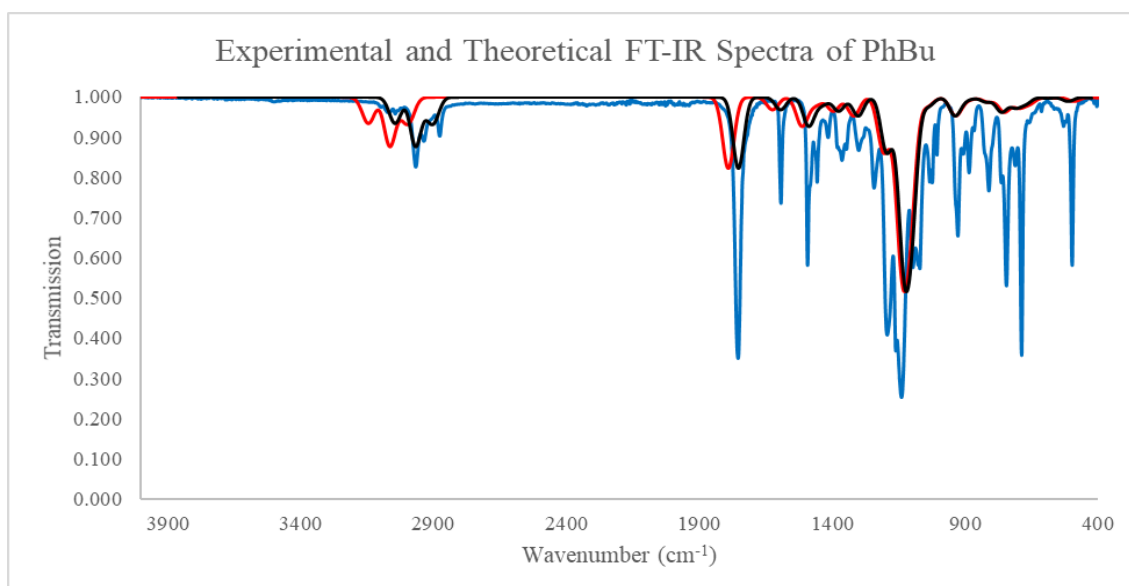


Figure 8. FT-IR Spectra of PhBu Experimental (Blue), Theoretical using B97-3c (Red), and B97-3c with Scaling Factors (Black)

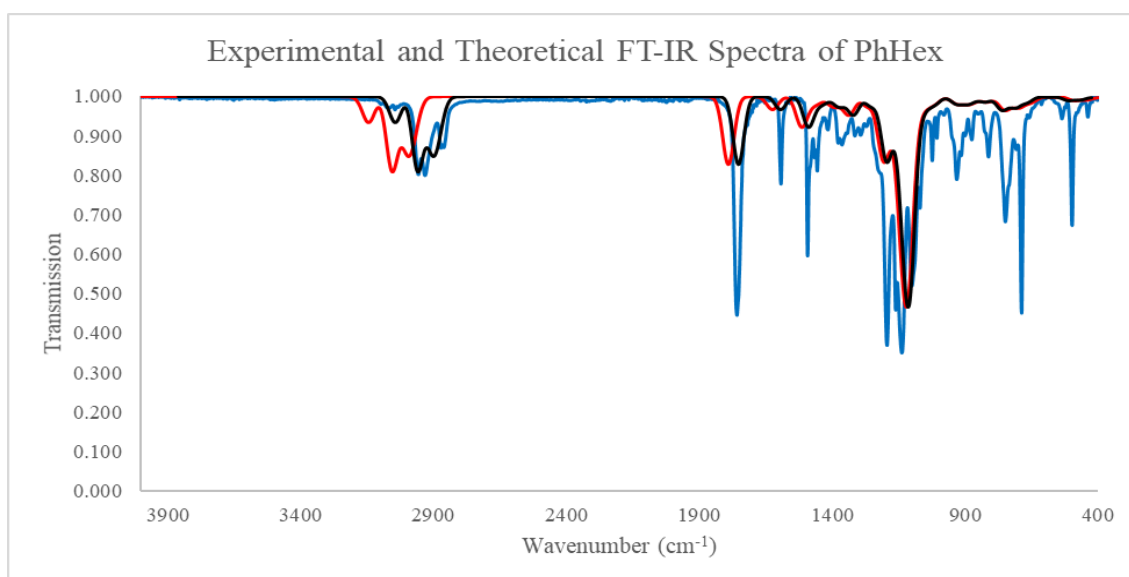
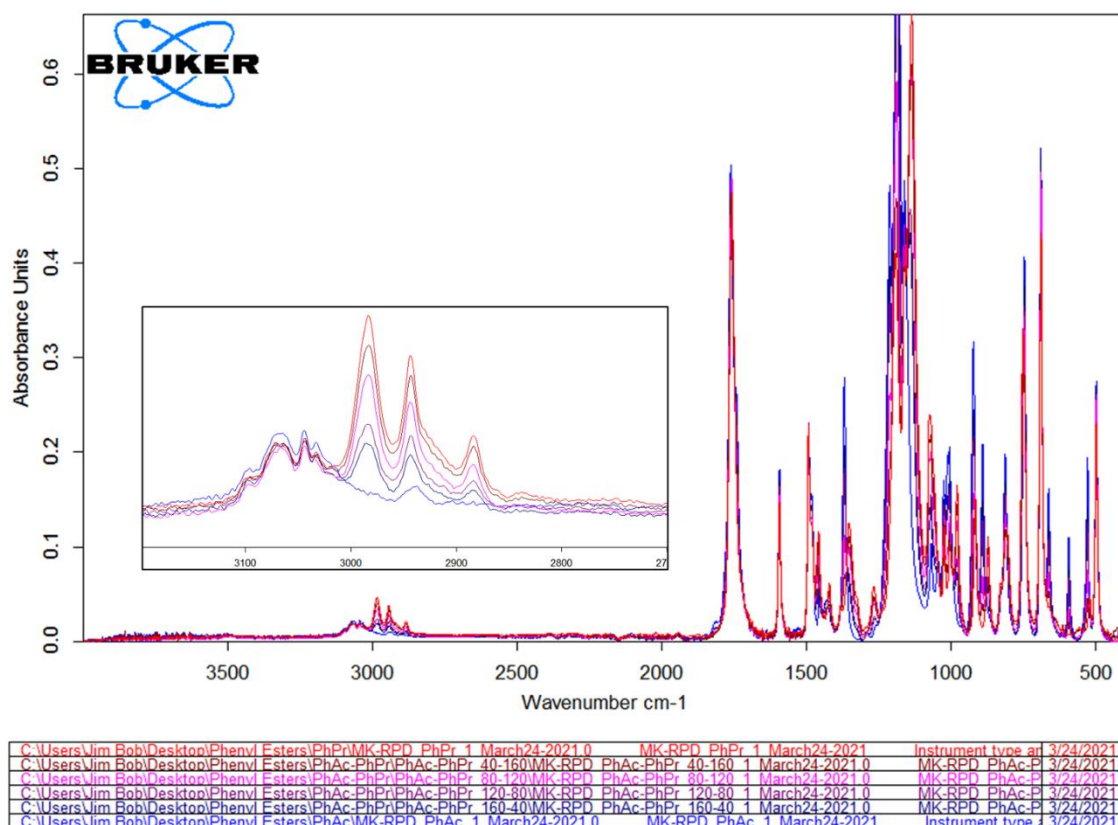
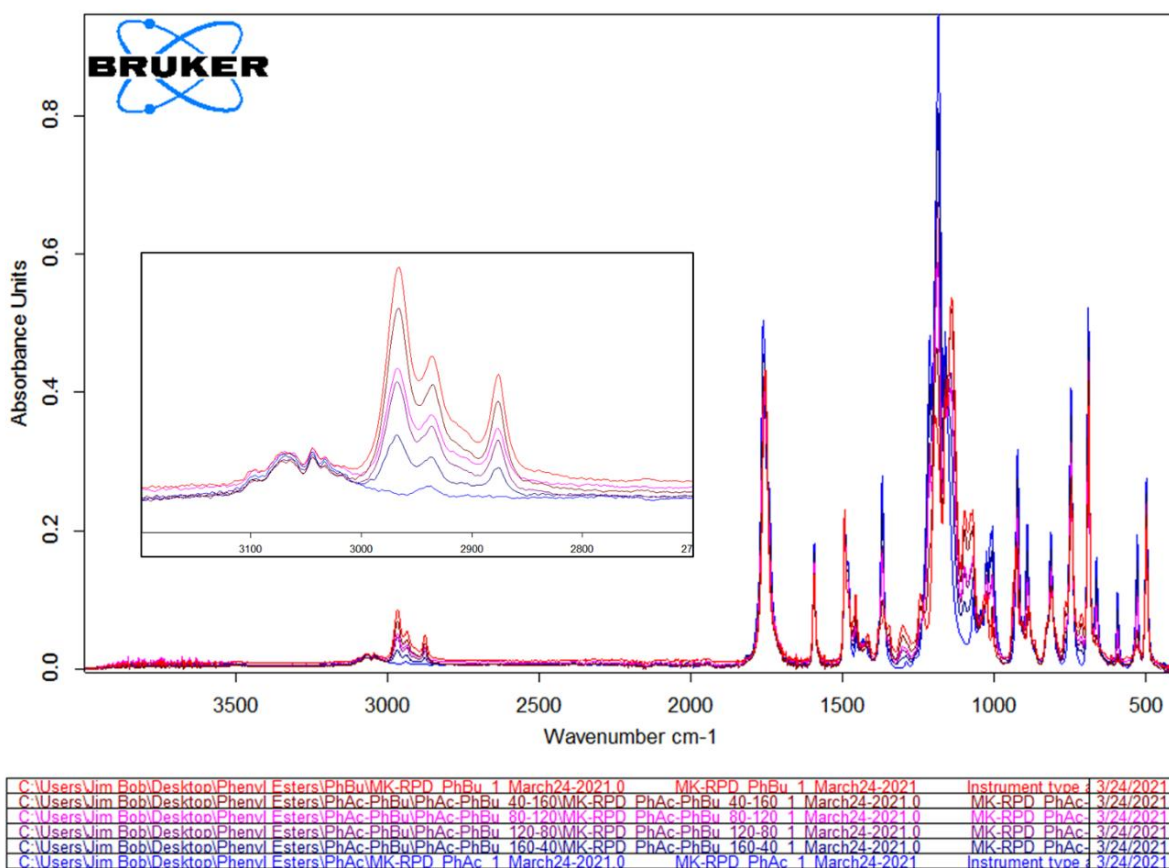


Figure 9. FT-IR Spectra of PhHex Experimental (Blue), Theoretical using B97-3c (Red), and B97-3c with Scaling Factors (Black)

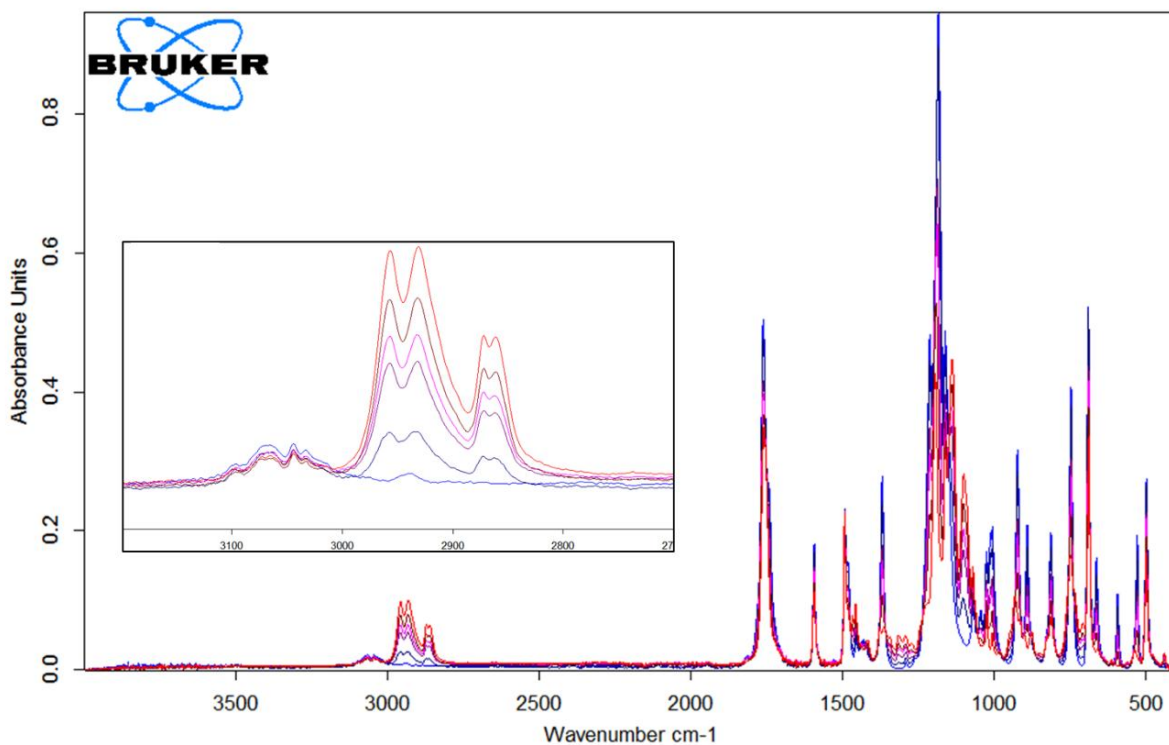


Page 1/1

Figure 10. FT-IR Spectra of PhAc-PhPr Mixtures with Zoomed-in Area between 3200-2700 cm^{-1} 

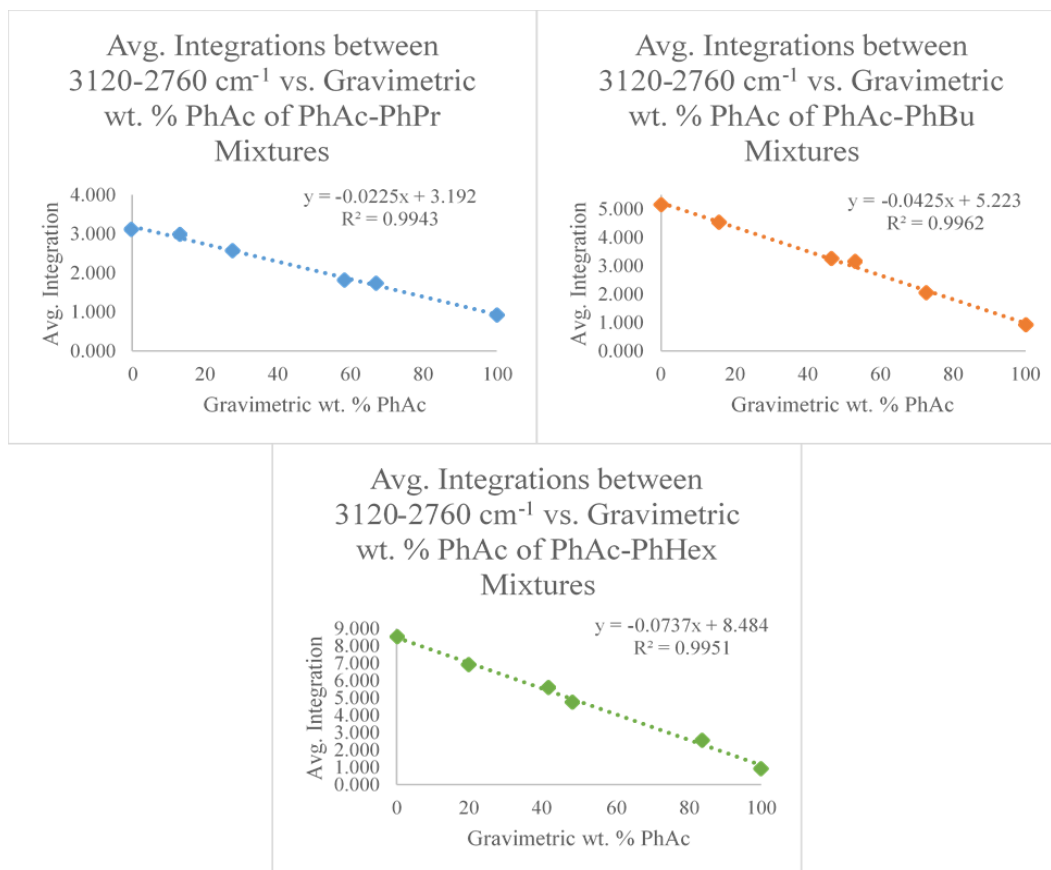
Page 1/1

Figure 11. FT-IR Spectra of PhAc-PhBu Mixtures with Zoomed-in Area between 3200-2700 cm^{-1}



C:\Users\Jim\Bob\Desktop\Phenyl Esters\PhHex\MK-RPD_PhHex_1_March24-2021.0	MK-RPD_PhHex_1_March24-2021	Instrument ty	3/24/2021
C:\Users\Jim\Bob\Desktop\Phenyl Esters\PhAc-PhHex\PhAc-PhHex_40-160\MK-RPD_PhAc-PhHex_40-160_1_March24-2021.0	MK-RPD_PhAc_1_March24-2021	MK-RPD_Ph	3/24/2021
C:\Users\Jim\Bob\Desktop\Phenyl Esters\PhAc-PhHex\PhAc-PhHex_80-120\MK-RPD_PhAc-PhHex_80-120_1_March24-2021.0	MK-RPD_PhAc_1_March24-2021	MK-RPD_Ph	3/24/2021
C:\Users\Jim\Bob\Desktop\Phenyl Esters\PhAc-PhHex\PhAc-PhHex_120-80\MK-RPD_PhAc-PhHex_120-80_1_March24-2021.0	MK-RPD_PhAc_1_March24-2021	MK-RPD_Ph	3/24/2021
C:\Users\Jim\Bob\Desktop\Phenyl Esters\PhAc-PhHex\PhAc-PhHex_160-40\MK-RPD_PhAc-PhHex_160-40_1_March24-2021.0	MK-RPD_PhAc_1_March24-2021	MK-RPD_Ph	3/24/2021
C:\Users\Jim\Bob\Desktop\Phenyl Esters\PhAc\MK-RPD_PhAc_1_March24-2021.0	MK-RPD_PhAc_1_March24-2021	Instrument type	3/24/2021

Page 1/1

Figure 12. FT-IR Spectra of PhAc-PhHex Mixture with Zoomed-in Area between 3200-2700 cm⁻¹Figure 13. Calibration Plots of Average Integrations between 3120-2760 cm⁻¹ vs. Gravimetric wt. % PhAc in PhAc-PhPr (Blue, Top Left), PhAc-PhBu (Orange, Top Right), and PhAc-PhHex (Green, Bottom Middle) Mixtures

3.4. qFT-IR Analysis of PhE Mixtures

All qFT-IR analyses were conducted using absorbance measurements. Figure 10 through Figure 12 showcase the overlapped FT-IR spectra of each PhE mixture. Peak integrations of each binary mixture were measured between 3120-2760 cm^{-1} , which consists of the aromatic and aliphatic $\nu\text{C-H}$ vibrations. Calibration plots of integrations vs. the gravimetric wt. % composition of PhAc were constructed. Figure 13 shows the calibration plots of the qFT-IR integrations vs. the gravimetric wt. % compositions of PhAc. All plots displayed a strong, linear correlation between the qFT-IR integration vs. the gravimetric wt. % composition of a component in each mixture. The R^2 values were greater than 0.99 in all cases.

Table 4. Summary of Experimental Wt. % PhAc of 50:50 Mixtures

50:50 Mixture	Gravimetric wt. % PhAc	Experimental wt. % PhAc	Experimental wt. % PhAc 95% CI
PhAc-PhPr	50.73	51.35	51.35 \pm 4.20
PhAc-PhBu	52.01	50.98	50.98 \pm 3.18
PhAc-PhHex	52.67	51.73	51.73 \pm 3.43

The experimental wt. % PhAc of the 50:50 mixtures obtained via qFT-IR analyses and the calibration plots are shown in Table 4. Gravimetric wt. % PhAc in all binary mixtures were within the 95% CI of their experimentally determined counterparts for five measurements.

4. Conclusions

This multi-part experiment demonstrates the qualitative and quantitative uses of FT-IR in the undergraduate laboratory. All FT-IR spectra of the synthesized PhEs agreed with those of their standards, databases, and theoretical counterparts. The constructed calibration plots can be used to accurately determine the wt. % composition of a component in a binary mixture using different PhEs. There is a strong, linear correlation between the FT-IR peak integrations and the wt. % composition of a component determined gravimetrically. This experiment can either be expanded to include other PhE mixtures or adapted for different reagents. Furthermore, it serves as an excellent tool for the undergraduate chemistry laboratory, one that combines four major branches of chemistry: computational, instrumental, organic, and analytical.

Acknowledgments

Special thanks to Joseph Mancuso and Brandon Khanyan who reviewed this article. We also acknowledge the support from a Hofstra University HCLAS Faculty Research and Development Grant.

List of Abbreviations

CI – Confidence Interval
 DFT – Density Functional Theory
 FT-IR – Fourier-Transform Infrared Spectroscopy

IR – Infrared Spectroscopy
 PhAc – Phenyl Acetate
 PhBu – Phenyl Butyrate
 PhEs – Phenyl Esters
 PhHex – Phenyl Hexanoate
 PhOH – Phenol
 PhPr – Phenyl Propionate
 qFT-IR – Quantitative FTIR
 R^2 – Correlation Coefficient
 Wt. % - Weight Percent
 δ – Bending Vibration
 ν – Stretching Vibration

References

- [1] Schuttlefield, J. D.; Grassian, V. H. ATR-FTIR Spectroscopy in the Undergraduate Chemistry Laboratory. Part I: Fundamentals and Examples. *J. Chem. Educ.* 2008, 85 (2), 279.
- [2] Robinson, J. W.; Frame, E. S.; Frame II, G. M. Chapter 4. In *Undergraduate Instrumental Analysis*; CRC Press: New York, 2014.
- [3] Conklin, A.; Goldcamp, M. J.; Barrett, J. Determination of Ethanol in Gasoline by FT-IR Spectroscopy. *J. Chem. Educ.* 2014, 91 (6), 889-891.
- [4] Gebel, M. E.; Kaleuati, M. A.; Finlayson-Pitts, B. J. Measurement of Organics Using Three FTIR Techniques: Absorption, Attenuated Total Reflectance, and Diffuse Reflectance. *J. Chem. Educ.* 2003, 80 (6), 672.
- [5] Lambert, J. B.; Gronet, S.; Shurvell, H. F.; Lightner, D. *Organic Structural Spectroscopy*, 2nd ed.; Prentice Hall: New Jersey, 2010.
- [6] Veening, H. Quantitative Infrared Analysis of Xylene Mixtures: Internal Standard Method. *J. Chem. Educ.* 1966, 43 (6), 319.
- [7] Silverstein, R. M.; Webster, F. X. *Spectrometer Identification of Organic Compounds*, 7th ed.; Wiley & Sons: New Jersey, 2011.
- [8] Smith, R. E., IV; McKee, J. R.; Zanger, M. The Electrophilic Bromination of Toluene: Determination of the Ortho, Meta, and Para Ratios by Quantitative FTIR Spectrometry. *J. Chem. Educ.* 2002, 79, 227.
- [9] Bellamy, M. K. Using FTIR-ATR Spectroscopy To Teach the Internal Standard Method. *J. Chem. Educ.* 2010, 87 (12), 1399-1401.
- [10] Tarhan, I.; Ismail, A. A.; Kara, H. Quantitative Determination of Free Fatty Acids in Extra Virgin Olive Oils by Multivariate Methods and Fourier Transform Infrared Spectroscopy Considering Different Absorption Modes. *Int. J. Food Prop.* 2017, 20 (sup1), S790-S797.
- [11] Ismail, A. A.; van de Voort, F. R.; Emo, G.; Sedman, J. Rapid Quantitative Determination of Free Fatty Acids in Fats and Oils by Fourier Transform Infrared Spectroscopy. *J. Am. Oil Chem. Soc.* 1993, 70 (4), 335-341.
- [12] Vongsvivut, J.; Heraud, P.; Zhang, W.; Kralovec, J. A.; McNaughton, D.; Barrow, C. J. Quantitative Determination of Fatty Acid Compositions in Micro-Encapsulated Fish-Oil Supplements Using Fourier Transform Infrared (FTIR) Spectroscopy. *Food Chem.* 2012, 135 (2), 603-609.
- [13] Christy, A. A.; Egeberg, P. K. Quantitative Determination of Saturated and Unsaturated Fatty Acids in Edible Oils by Infrared Spectroscopy and Chemometrics. *Chemom. Intell. Lab. Syst.* 2006, 82 (1), 130-136.
- [14] Al-Alawi, A.; van de Voort, F. R.; Sedman, J.; Ghetler, A. Automated FTIR Analysis of Free Fatty Acids or Moisture in Edible Oils. *JALA J. Assoc. Lab. Autom.* 2006, 11 (1), 23-29.
- [15] Mahesar, S. A.; Kandhro, A. A.; Khaskheli, A. R.; Talpur, M. Y.; Sherazi, S. T. H. SB-ATR FTIR Spectroscopic Monitoring of Free Fatty Acids in Commercially Available Nigella Sativa (Kalonji) Oil. *J. Spectrosc.* 2014, 2014, e510890.
- [16] Koca, N.; Rodriguez-Saona, L. E.; Harper, W. J.; Alvarez, V. B. Application of Fourier Transform Infrared Spectroscopy for Monitoring Short-Chain Free Fatty Acids in Swiss Cheese. *J. Dairy Sci.* 2007, 90 (8), 3596-3603.
- [17] Franck, P.; Sallerin, J. L.; Schroeder, H.; Gelot, M. A.; Nabet, P. Rapid Determination of Fecal Fat by Fourier Transform Infrared

- Analysis (FTIR) with Partial Least-Squares Regression and an Attenuated Total Reflectance Accessory. *Clin. Chem.* 1996, 42 (12), 2015-2020.
- [18] Marina, A. M.; Wan Rosli, W. I.; Noorhidayah, M. Rapid Quantification of Free Fatty Acids in Virgin Coconut Oil by FTIR Spectroscopy. *Malays. Appl. Biol.* 2015, 44 (2), 45-49.
- [19] D'Amelia, R. P.; Gentile, S.; Nirode, W. F.; Huang, L. Quantitative Analysis of Copolymers and Blends of Polyvinyl Acetate (PVAc) Using Fourier Transform Infrared Spectroscopy (FTIR) and Elemental Analysis (EA). *World J. Chem. Educ.* 2016, 4 (2), 25-31.
- [20] D'Amelia, R. P.; Huang, L.; Mancuso, J. Quantitative Analysis of Polyvinyl Alcohol-Polyethylene (PVOH-PE) Copolymers and Polyvinyl Pyrrolidone-Polyvinyl Acetate (PVP-PVAc) Copolymers and Blends Using Fourier Transform Infrared Spectroscopy and Elemental Analysis. *World J. Chem. Educ.* 2019, 7 (1), 1-11.
- [21] Guerrero-Pérez, M. O.; Patience, G. S. Experimental Methods in Chemical Engineering: Fourier Transform Infrared Spectroscopy-FTIR. *Can. J. Chem. Eng.* 2020, 98 (1), 25-33.
- [22] Stuart, B. Infrared Spectroscopy. In *Kirk-Othmer Encyclopedia of Chemical Technology*; American Cancer Society, 2015; pp 1-18.
- [23] Sadjadi, S.; Zhang, Y.; Kwok, S. A THEORETICAL STUDY ON THE VIBRATIONAL SPECTRA OF POLYCYCLIC AROMATIC HYDROCARBON MOLECULES WITH ALIPHATIC SIDEGROUPS. *Astrophys. J.* 2015, 801 (1), 34.
- [24] Zhao, N.; Lamichanne, H. P.; Hastings, G. Comparison of Calculated and Experimental Isotope Edited FTIR Difference Spectra for Purple Bacterial Photosynthetic Reaction Centers with Different Quinones Incorporated into the QA Binding Site. *Front. Plant Sci.* 2013, 4.
- [25] Parlak, C.; Ramasami, P. Theoretical and Experimental Study of Infrared Spectral Data of 2-Bromo-4-Chlorobenzaldehyde. *SN Appl. Sci.* 2020, 2 (7), 1148.
- [26] A. Basiuk, V. IR Spectra Simulation as Auxiliary Tool for Gas Chromatography-Fourier Transform IR Spectroscopy-Mass Spectrometry Identification of Unknown Compounds: Comparison between Several Semi-Empirical Methods. *Spectrochim. Acta. A. Mol. Biomol. Spectrosc.* 1999, 55 (2), 289-298.
- [27] Alves, R. M.; Rodembusch, F. S.; Habis, C.; Moreira, E. C. FT-Raman and FTIR Spectra of Photoactive Aminobenzazole Derivatives in the Solid State: A Combined Experimental and Theoretical Study. *Mater. Chem. Phys.* 2014, 148 (3), 833-840.
- [28] Umar, Y.; Abu-Thabit, N.; Jerabek, P.; Ramasami, P. Experimental FTIR and Theoretical Investigation of the Molecular Structure and Vibrational Spectra of Acetanilide Using DFT and Dispersion Correction to DFT. *J. Theor. Comput. Chem.* 2019, 18 (02), 1950009.
- [29] Katsyuba, S. A.; Zvereva, E. E.; Grimme, S. Fast Quantum Chemical Simulations of Infrared Spectra of Organic Compounds with the B97-3c Composite Method. *J. Phys. Chem. A* 2019, 123 (17), 3802-3808.
- [30] Alecu, I. M.; Zheng, J.; Zhao, Y.; Truhlar, D. G. Computational Thermochemistry: Scale Factor Databases and Scale Factors for Vibrational Frequencies Obtained from Electronic Model Chemistries. *J. Chem. Theory Comput.* 2010, 6 (9), 2872-2887.
- [31] Kesharwani, M. K.; Brauer, B.; Martin, J. M. L. Frequency and Zero-Point Vibrational Energy Scale Factors for Double-Hybrid Density Functionals (and Other Selected Methods): Can Anharmonic Force Fields Be Avoided? *J. Phys. Chem. A* 2015, 119 (9), 1701-1714.
- [32] Gastegger, M.; Behler, J.; Marquetand, P. Machine Learning Molecular Dynamics for the Simulation of Infrared Spectra. *Chem. Sci.* 2017, 8 (10), 6924-6935.
- [33] Selzer, P. IR Spectra Simulation and Information Processing on the WWW. *Chim. Int. J. Chem.* 1998, 52 (11), 678-682.
- [34] Qiao, Z.; Welborn, M.; Anandkumar, A.; Manby, F. R.; Miller, T. F. OrbNet: Deep Learning for Quantum Chemistry Using Symmetry-Adapted Atomic-Orbital Features. *J. Chem. Phys.* 2020, 153 (12), 124111.
- [35] Hanwell, M. D.; Curtis, D. E.; Lonie, D. C.; Vandermeersch, T.; Zurek, E.; Hutchison, G. R. Avogadro: An Advanced Semantic Chemical Editor, Visualization, and Analysis Platform. *J. Cheminformatics* 2012, 4 (1), 17.
- [36] Avogadro: An Open Source Molecular Builder and Visualization Tool. Version 1.2.0 (with ORCA Support); University of Pittsburgh: Pittsburgh, PA, 2018.
- [37] Rappe, A. K.; Casewit, C. J.; Colwell, K. S.; Goddard, W. A.; Skiff, W. M. UFF, a Full Periodic Table Force Field for Molecular Mechanics and Molecular Dynamics Simulations. *J. Am. Chem. Soc.* 1992, 114 (25), 10024-10035.
- [38] Neese, F.; Wennmohs, F.; Becker, U.; Riplinger, C. The ORCA Quantum Chemistry Program Package. *J. Chem. Phys.* 2020, 152 (22), 224108.
- [39] Brandenburg, J. G.; Bannwarth, C.; Hansen, A.; Grimme, S. B97-3c: A Revised Low-Cost Variant of the B97-D Density Functional Method. *J. Chem. Phys.* 2018, 148 (6), 064104.
- [40] National Institute of Advanced Industrial Science and Technology (AIST): Spectral Database for Organic Compounds (SDBS) <https://sdfs.db.aist.go.jp> (accessed Apr 12, 2021).

